Age-dependent high-yield isolation of primordial, primary, and early secondary follicles from the bovine ovarian cortex

Noemi Monferini*, Pritha Dey*, Ludovica Donadini, Niki Katsakoglou, Federica Franciosi, Valentina Lodde, and Alberto Maria Luciano[1]

Reproductive and Developmental Biology Laboratory (ReDBioLab), Department of Veterinary Medicine and Animal Sciences, University of Milan, Milan, Italy.

*These authors contributed equally

[1]Correspondence: Alberto M. Luciano, Dipartimento di Medicina Veterinaria e Scienze Animali, Università degli Studi di Milano, Via dell'Università, 6 - 26900 Lodi, Italy - Phone (+39) 02 50334348 - alberto.luciano@unimi.it

Running title: Bovine preantral follicle isolation

In brief: Preantral follicles constitute the largest follicle reserve in the mammalian ovary. This study assesses a mechanical isolation method to maximize the number of follicles retrieved from a defined cortex volume.

Key Words

Ovary, Preantral follicles, Folliculogenesis, Fertility preservation, Follicle reserve, Aging

Abstract

Primordial, primary, and secondary follicles (collectively defined as preantral follicles) constitute the most abundant source of gametes inside the mammalian ovarian cortex. The massive isolation of preantral follicles and the refinement of stage-specific protocols for in vitro follicle growth would provide a powerful tool to boost the rescue and restoration of fertility in assisted reproduction interventions in human medicine, animal breeding, and vulnerable species preservation. Nevertheless, together with an efficient culture system, the most significant limitation to implementing in vitro follicle growth is the lack of an efficient method to isolate viable and homogeneous sub-populations of primordial, primary, and secondary follicles suitable for in vitro culture. Our study provides a strategy for high-yielding mechanical isolation of primordial, primary, and early secondary follicles from a limited portion of the ovarian cortex in the bovine animal model.

In the first part of the study, we refined a mechanical isolation protocol of preantral follicles, adopting specific methodological strategies to separate viable and distinct sub-populations of primordial (oblate and prolate forms), primary, and early secondary follicles from 0.16 cm^3 of the ovarian cortex. In the second part of the study, we tested the effectiveness of the isolation protocol, considering the individual's age as a critical factor, bearing in mind the progressive decrease in the ovarian reserve that naturally accompanies the reproductive lifespan.

Our study provides a way for designing quantitative and conservative fertility preservation approaches to preserve organ function and minimize the invasiveness of the interventions, also considering age-related differences.

Introduction

The mammalian ovary is a considerable source of oocytes established during fetal life and organized into follicles. These follicles represent the ovarian reserve that declines with age up to the end of the reproductive lifespan (Ford, et al. 2020). The number of follicles in the ovaries of mammals is remarkably variable at birth, ranging from 350,000 to 1,100,000 in humans (Forabosco and Sforza 2007, Gougeon, et al. 1994) and approximately 14,000 to 250,000 in cattle (Erickson 1966a, b, Silva-Santos, et al. 2011).

Folliculogenesis begins during fetal life, and at puberty, the cyclic recruitment of primordial follicles leads to the development of the preovulatory follicle containing an oocyte, which is ovulated and can become an embryo after fertilization (McGee and Hsueh 2000). Only a few follicles of the initial pool are recruited to grow to reach the preovulatory stage. Less than 1% escape atresia at various stages of development, particularly during the preantral to early antral transition, which is the most susceptible period to this process (Luciano and Sirard 2018, McGee and Hsueh 2000). During a woman's reproductive lifespan, of the original primordial follicle stockpile at birth, only approximately 400 will fully mature into secondary oocytes, be released in the fallopian tube through ovulation, and be ready for fertilization (Findlay, et al. 2015, Hansen, et al. 2008) while the vast majority are fated to undergo atresia (Dey and Luciano 2022, Marcozzi, et al. 2018, Tilly 2001).

Primordial, together with primary and secondary follicles (collectively defined as preantral follicles), account for the high majority of follicles in the ovarian cortex (Rodgers and Irving-Rodgers 2010b) and represent the largest population of the ovarian reserve in mammals at any given time, thus constituting the most significant repository of the female reproductive potential in mammals (Bus, et al. 2019, Telfer 2019).

Developing efficient culture systems for preantral follicles could enhance fertility preservation prospects in women undergoing ovarian cortical tissue harvesting, expand genetically important livestock breeds, and support conservation programs for threatened species (Xu and Zelinski 2022). In fact, the current assisted reproductive technologies (ARTs) in

mammals rely only on the narrow population of fully-grown oocytes isolated from medium-large antral follicles, which in the bovine are about a dozen per ovary (Lonergan and Fair 2008, Luciano, et al. 2021, Luciano, et al. 2018) and, with lower success, from growing oocytes isolated from early antral follicles (Garcia Barros, et al. 2023).

In vitro preantral follicle growth systems have been attempted in several species in the last three decades (Simon, et al. 2020). Despite some advances in current methods, success was limited to mice (O'Brien, et al. 2003), with "Eggbert" as proof of principle, while in large mammals, the techniques are still considered experimental (Araujo, et al. 2014, Simon, et al. 2020, Telfer, et al. 2019). While promising two- and three-dimensional culture systems to mimic the ovarian environment have recently been proposed in mice (Converse, et al. 2023) and humans (Grubliauskaite, et al. 2024), several restraints persist in developing an in vitro culture system.

A significant limitation to the full exploitation of the ovarian reserve is the lack of efficient methods for isolating homogeneous populations of preantral follicles. The available isolation techniques, mechanical, enzymatic, or in combination (Figueiredo, et al. 1993, Hornick, et al. 2013, Langbeen, et al. 2015) are poised by poor yields and often allow the isolation only of primary and secondary follicles (Araujo, et al. 2015, Barboni, et al. 2011, Barros, et al. 2019, Bezerra, et al. 2019, Candelaria and Denicol 2020, Candelaria, et al. 2020, McDonnell, et al. 2022), most of the time obtained by processing several whole fetal or newborn ovaries (Amin, et al. 2013, Figueiredo, et al. 1993, Hulshof, et al. 1994, Lazzari, et al. 1992, Santos, et al. 2013). Yields obtained from adult individuals are even lower and recurrently require processing a high number of ovaries or a large amount of ovarian tissue (Dolmans, et al. 2006, Figueiredo, et al. 1993, Langbeen, et al. 2015, Langbeen, et al. 2014, McDonnell, et al. 2022, Vanacker, et al. 2011). While the yield rate per individual is reported only in a few cases, whenever available, the number of follicles recovered is so exiguous that it is difficult to contextualize the procedure into a personalized approach in fertility rescue. Designing an intervention scheme based on the population of follicles present in a certain amount of ovarian cortex lays the foundation for fertility preservation programs.

The objective of our study was to contribute a framework for designing the rationale of quantitative and conservative interventions in fertility preservation programs, taking into account the physiological decline of the ovarian reserve accompanying the reproductive lifespan. The first part of the study aimed to refine a mechanical isolation protocol of preantral ovarian follicles. The second part of the study aimed to define the effectiveness of the isolation protocol, accompanied by histologic and morphometric evaluation considering the individual's age as a critical factor, bearing in mind the progressive decrease in the ovarian reserve that naturally accompanies the reproductive lifespan. Our findings provide a high-yield strategy for designing quantitative and conservative fertility preservation treatment from an age-related perspective while giving tools to decipher molecular mechanisms guiding folliculogenesis processes and laying the foundations to implement follicle-stage specific in vitro growth systems.

Materials and methods

All chemicals and reagents used in this study were purchased from Merck Sigma Aldrich, Italy, except those specifically mentioned. Disposable sterile plasticware was purchased from SARSTEDT Srl, Italy (SARSTEDT Green line for suspension cells) and Thermo Fisher Scientific Inc, Germany (NUNC IVF Line and Sterilin^{TM}). All the procedures were conducted at room temperature (26°C) unless otherwise specified.

Ovary collection

Holstein Friesian bovine ovaries were recovered at a local abattoir (IT 2270M CE; Inalca S.p.A., Ospedaletto Lodigiano, LO, Italy) from pubertal dairy cows (1-8 years old) subjected to routine veterinary inspection and according to the specific health requirements. Only animals with both ovaries with more than 10 mid-antral follicles (2-8 mm) visible on the ovarian surface (Modina, et al. 2014) were considered. For each animal, ovary pairs were stripped of surrounding fat tissue and ligaments and transferred into a 50 mL tube in sterile saline (NaCl, 9 g/L), supplemented with penicillin 100 U/mL and streptomycin 0.1 mg/mL (pen/strep). Ovaries were transported to the laboratory at 4°C within 1 hour and kept cold until processing to minimize ovarian tissue damage (Duncan, et al. 2016, Vilela, et al. 2021). Ovaries isolated from 12 to 24-month-old heifers and from 40 to 87-month-old cows were collected to evaluate the effect of age on preantral follicle density, follicle isolation yield rate, and recovery efficiency (Erickson 1966b, Silva-Santos, et al. 2011). One ovary per animal was randomly selected to conduct the analyses.

Preantral follicle isolation

Preantral follicles were isolated as previously described for the primordial follicles (Dey, et al. 2024) and modified as illustrated in Fig. 1 and described below. Each ovary was washed twice in pen/strep saline, measured, and weighed. The ovary was placed on a sterile cutting

144 board, and an ovarian cortex strip with an area of 10x20 mm and thickness between 0.5-1
145 mm (approximately 0.1-0.2 cm^3) was cut using a ruler and a surgical blade mounted on a
146 scalpel handle (Supplementary Fig. 1). Notably, we took into consideration a depth of
147 ovarian tissue which would mainly contain follicles from the primordial up to the early
148 secondary (van Wezel and Rodgers 1996). The cortical strip was chopped into smaller
149 fragments with 1.5" single-edge razor blades and carefully minced on a sterile cutting board.
150 Minced ovarian cortex was washed by transferring the pieces with a spatula into a sterile 60
151 mm Petri dish containing 3 mL of Leibovitz's L-15 Medium supplemented with 3 mg/mL
152 Bovine Serum Albumin and pen/strep (isolation medium). After removing the isolation
153 medium using a pipette, minced cortical pieces were transferred into a 50 mL tube
154 containing 15 mL of isolation medium. The 50 mL tube containing the minced cortical pieces
155 was placed under an IKA ULTRA-TURRAX® T25 Homogenizer (IKA-Werke, Germany) with
156 the Dispersing Tool S25D-14G-KS (IKA-Werke) and fragments were homogenized at 3000
157 rpm for 6 minutes. The homogenate was passed through a 300 µm mesh size strainer
158 (pluriSelect Life Science, Germany) placed on top of a 50 mL tube, and the strainer mesh
159 was washed with 5 mL of isolation media. The filtrate was then serially passed through 100,
160 70, 40, and 30 µm mesh size strainers placed atop a 50 mL tube, and each strainer was
161 washed with 5 mL of isolation media. Based on their diameter, primordial, primary, and early
162 secondary follicles were trapped by 30, 40, and 70 µm mesh size strainers, respectively.
163 Each strainer was flipped upside-down and stably hovered over a 60 mm Petri dish.
164 Entrapped follicles were then flushed out by washing the strainer with 5 mL of isolation
165 medium. Under a high-zoom ratio stereomicroscope (Nikon SMZ1270i, Nikon, Japan)
166 equipped with a DSFi3 camera and with NIS Elements L image analysis (Nikon, Japan).
167 Primordial, primary, and secondary follicles were isolated from the resultant filtrate with a
168 mouth pipette with a pulled glass capillary (inner diameter about 100 µm) and transferred
169 into a 35 mm Petri dish with 2 mL of isolation medium. Follicles from each category were
170 placed in a 4-well plate containing 500 µL of culture medium, which was αMEM with
171 nucleosides and GlutaMAX™, supplemented with 1 mg/mL Bovine Serum Albumin fatty

acid-free, 1mg/mL r-hInsulin, 0.55 mg/mL hTransferrin, 0.5 µg/mL Sodium Selenite, 10^{-4} IU/mL r-hFSH, and pen/strep. This medium has been demonstrated to be effective in better preserving the morphology, morphometry, and ultrastructure of pre-antral follicles, ensuring their survival and growth (Bjarkadottir, et al. 2021, Jachter, et al. 2022, Jimenez, et al. 2016, Wright, et al. 1999). Follicles were incubated for 1 hour at 38.5°C with 5% CO_2 in the air and maximum humidity.

All the procedures were completed within 30-45 minutes per ovary to prevent follicle suffering and loss since they become sticky and degenerate if kept for prolonged periods outside of the incubator, as also recently reported in mice (Converse, et al. 2023) and bovine (McDonnell, et al. 2022).

Morphological characterization and viability assessment of isolated early preantral follicles

After 1 hour of incubation in the αMEM-based culture medium, groups of freshly isolated follicles were observed under an inverted light microscope (Nikon Diaphot-TMD Inverted Microscope, Nikon, Japan) equipped with a Nikon DS-L1 camera (Nikon, Japan) for image acquisition and to subsequently evaluate their morphology. The follicles were classified following the morphological features previously described as "primordial oblate" or spherical when the oocyte was surrounded by one layer of flattened pre-granulosa cells and as "primordial prolate" or ellipsoid (Rodgers and Irving-Rodgers 2010b, van Wezel and Rodgers 1996). The two shapes of primordial follicles are also reported in humans and rats and described with the terms intermediate or transition (Gougeon and Chainy 1987, Meredith, et al. 2000, Rodgers and Irving-Rodgers 2010b) when clustering flat granulosa cells at two opposite poles on the axis of the follicle and at least one cuboidal granulosa cell. Follicles were classified as "primary" when one complete layer of cuboidal granulosa cells surrounded the oocyte and as "early secondary" follicles characterized by two or three layers of cuboidal granulosa cells (Candelaria and Denicol 2020, Hulshof, et al. 1994, Langbeen, et

al. 2015). Follicles diameter was determined by averaging three diameters (horizontal, vertical, and diagonal) of each follicle on digital images using NIH ImageJ 1.54h (Rueden, et al. 2017, Schneider, et al. 2012).

Follicle viability was assessed using a dual-fluorescence viability assay prepared with Fluorescein Diacetate (FDA) and Propidium Iodide (PI) diluted to a final concentration of 1 µg/mL each in Polyvinyl Alcohol dissolved in Phosphate Buffer Saline to a final concentration of 0.1% (PBS/PVA, manipulation buffer). Groups of 5 to 10 follicles were washed in a 50 µL drop of manipulation buffer and then transferred in a 50 µL drop of dual staining solution. After one minute of incubation, follicles were observed at appropriate wavelengths under a fluorescence microscope (Nikon Diaphot-TMD Inverted Microscope with fluorescent filter DM 510) equipped with a Nikon DS-L1 camera for digital image acquisition. As previously categorized, follicles were classified as viable when the oocyte and all the granulosa cells were alive (green fluorescence) or when with < 10% of dead granulosa cells (red fluorescence) (Dolmans, et al. 2006).

Histology and morphometry

Qualitative and quantitative morphological analyses were performed on biopsy punches of the ovarian cortex following the protocol recently adopted in William's lab (Adeniran, et al. 2021) for ovarian tissue from humans, sheep, and mice, which in the present work has been extended to bovine species. The protocol was developed to improve morphological preservation, thus reducing biased evaluation of stroma organization and follicle developmental stages, amongst other histological criteria, and successfully supporting downstream assays, such as immunohistochemical staining in ovarian tissue from multiple species.

Tissue processing and staining

Tissue biopsies were randomly excised from 20x10 mm in size and 0.5 to 1 mm thick ovarian cortex strips prepared as described above, using 2 mm sterile biopsy punches (Kay Medical, Japan) (Supplementary Fig. 1), washed in sterile PBS and then randomly assigned to neutral buffered formalin (NBF) with 5% acetic acid (referred to hereafter as Form-Acetic fixative) (Adeniran, et al. 2021) and to our standard protocol using NBF (Luciano, et al. 2011, Modina, et al. 2014, Tessaro, et al. 2011). The volume of the fixative was at least 10 times more than the volume of the sample. Samples were fixed in the two conditions for 16 and 24 hours at room temperature and subjected to gentle rocking.

Post fixation, ovarian cortex biopsies were washed in sterile PBS and processed with the same tissue dehydration protocol with increasing ethanol concentrations (70%, 80%, 90%, 100%, three times each), cleared with two passages in ethanol 100% and xylene (1:1) and three times in xylene, then embedded in paraffin wax. Ovarian cortex biopsies were embedded in paraffin blocks, being careful that the orientation of the sample was in its cross-section to visualize both cortex and medulla-oriented regions. All samples were serially sectioned at 6 µm.

Sections were stained with hematoxylin and eosin (H&E; Hematoxylin Gill no 1, Eosin Plus alcoholic solution, Bio-Optica, Milan, Italy). Briefly, sections were dewaxed in xylene two times and rehydrated in decreasing ethanol concentrations (100%, 95%, 90%, 80%, 70%) before staining. Sections were incubated in hematoxylin for 3 minutes, washed for 5 minutes in water, followed by a brief incubation in eosin for 6 seconds before dehydrating in ethanol (70%, 80%, 90%, 95%, and 100%) and clearing in xylene two times.

Stained slides were mounted using Bio-Mount HM mounting media (Bio-Optica, Milan, Italy) and examined under a light microscope (Nikon Eclipse E600, Nikon, Japan) with a Nikon DS-F12 digital camera. Images were captured at 20X magnification using the NIS-Elements L image analysis software using the same camera parameter setting.

Histological artifact assessment

Artifact assessments were performed on H&E-stained sections to determine the morphological integrity of ovarian tissue after fixation, involving assessing stroma integrity (space between stromal cells), follicle and follicle-stroma integrity (the amount of clear space because of cellular shrinkage due to fixation, and space between the follicle and the surrounding stroma, respectively), as previously described (Adeniran, et al. 2021). Stroma integrity was determined on digital images by measuring the total area of artifact within the stroma as a percentage of the total stroma area for each section analyzed, using thresholding on ImageJ NIH. Thresholding involved the conversion of RGB images to 8-bit grayscale type, carried out for all sections. Threshold values were adjusted using the original color image as a reference to discriminate artifacts from stained tissue regions. Spaces due to blood vessels and follicles were excluded from the stroma integrity analysis. Follicles from the primordial to the secondary stage were assessed for follicle integrity. Follicle integrity was determined by counting the follicles with artifacts as a percentage of the total number of follicles evaluated. Follicle and follicle-stroma artifacts were identified as detachment of follicle basal membrane from the stroma, shrinkage of ooplasm, and chromatin condensation of nuclei (Adeniran, et al. 2021). To avoid double counting, only follicles with a visible oocyte nucleus or nuclear membrane were included in this assessment every 30 µm. Sections selected for analysis were distributed throughout the tissue. All sections were assessed blindly by three operators.

Histological ovarian follicle classification

Follicles were classified according to established criteria (Fair, et al. 1997, Ireland, et al. 2008) and subclassified as follows. The population of primordial follicles was subclassified into primordial oblate and prolate follicles. Primordial oblate follicles were characterized by the presence of an oocyte surrounded by one layer of flattened pre-granulosa cells, while primordial follicles with clustered flat granulosa cells at two opposite poles along the axis of the follicle and at least one cuboidal granulosa cell were characterized as primordial prolate follicles (Rodgers and Irving-Rodgers 2010b, van Wezel and Rodgers 1996). Follicles were

classified as primary when one complete layer of cuboidal granulosa cells surrounded the oocyte, and early secondary follicles were characterized by two or three layers of cuboidal granulosa cells.

Follicles were considered morphologically healthy if they exhibited all the following criteria: an intact basal membrane, organized granulosa cell layers with occasional pyknotic granulosa cell nuclei, and an intact oocyte and nucleus. Follicles were considered atretic when showing multiple signs of atresia, such as eosinophilia of the ooplasm, contraction, clumping of the chromatin material, and wrinkling of the nuclear membrane (Ireland, et al. 2008, Modina, et al. 2014, Walker, et al. 2021). Using ImageJ NIH on digital images, the follicle, oocyte, and oocyte nucleus diameters were assessed by calculating the mean of two perpendicular and diagonal measurements. Only follicles that contained a cross-section of the oocyte nucleus were evaluated. All assessments were conducted anonymously by three operators.

Evaluation of follicle density and yield rate

The overall thickness of the ovarian cortical strips was calculated by measuring the height of the biopsies conducted in each animal used in the experiments. The height has been estimated as the average of three measurements conducted at three equidistant points of the longitudinal histological section of the biopsy.

Follicle counting was assessed in every tissue section, and each follicle was followed through neighboring sections to avoid double counting. To determine the tissue volume, the area of every 12th tissue section was measured using ImageJ NIH on digital images as previously described (Bjarkadottir, et al. 2021). Average area measurements were utilized to calculate the volume of each tissue piece. Follicle density, expressed as the number of follicles/mm^3, was determined by dividing the total number of follicles counted in serial sections by the tissue volume.

The yield rate was calculated by dividing the number of follicles isolated utilizing the mechanical procedure for the volume of cortex processed (10x20x0.8 mm, 0.16 cm^3) and

then expressed in 1 mm^3 in the two age groups. The recovery efficiency was estimated by proportionating the number of follicles isolated with follicular density.

Statistical analysis

All experiments were repeated at least three times. All statistical analyses were performed using GraphPad Prism version 10.1.1 (GraphPad Software, Boston, Massachusetts USA, www.graphpad.com). Normality tests were run to assess normal data distribution. Stroma integrity, follicle, oocyte, and oocyte nucleus diameters were analyzed using the Kruskal-Wallis test, followed by Dunn's multiple comparisons test; follicle integrity was analyzed with one-way ANOVA, followed by Tukey's test. Data are presented as mean ± SEM, and statistical significance was defined as $P < 0.05$.

Follicle recovery rate after mechanical isolation and follicle counts in serial sections, comparing heifers and cows, were analyzed with 2-way ANOVA followed by Šidák's test. Data are presented as mean ± SD, and statistical significance was defined as $P < 0.05$.

Results

Effect of mechanical isolation protocol on preantral follicle morphology and viability

In the first part of the study, ovarian cortical strips measuring 20x10 mm and 0.5-1 mm deep were subjected to mechanical isolation as described above. Follicle morphology and viability were assessed on 12 animals in three independent experiments. The serial filtrations with decreasing mesh size allowed for isolating homogeneous populations of preantral follicle sub-classes with minimum debris. Morphological analysis was conducted on 448 freshly isolated preantral follicles. As reported in Fig. 2 and Supplementary Table 1, the mechanical protocol isolates distinct categories of follicles, characterized by significantly increasing size, from primordial to early secondary follicle stage. Both primordial follicles, oblate and prolate shape (van Wezel and Rodgers 1996), were isolated from the homogenate. Primordial oblate follicles presented a single layer of flattened pre-granulosa cells surrounding the oocyte with a mean follicle diameter of 34.51 ± 3.79 µm (Fig. 2A, E), and primordial prolate follicles were characterized by flattened pregranulosa cells and at least one cuboidal granulosa cell with a mean diameter of 37.59 ± 3.97 µm (Fig. 2B, E). Both primordial oblate and prolate follicles were collected mainly in the 30 µm mesh strainer, even if prolate primordial follicles could also be found trapped in the 40 µm strainer due to the ellipsoidal shape (van Wezel and Rodgers 1996). Primary follicles were characterized by a complete layer of cuboidal granulosa cells and an average diameter of 47.63 ± 9.71 µm (Fig. 2C, E) and were mainly retrieved in the 40 µm mesh strainer. Early secondary follicles were characterized by two to three layers of granulosa cells and a mean diameter of 75.9 ± 16.4 µm (Fig. 2D, E) and retrieved in the 70 µm mesh strainer and occasionally in the 40 µm mesh strainer.

Viability was assessed on 283 primordial, 117 primary, and 37 early secondary follicles after one hour of incubation for recovery (Fig. 3). Upon observation under fluorescence microscopy, follicles were classified into two categories depending on the percentage of dead granulosa cells and oocyte viability (Walker, et al. 2021). The overall

preantral follicle population viability was 68%, higher in primordial follicles (84.7%) than in primary (54.1%) and early secondary follicles (63.8%) (Fig 3C). No differences in viability were observed between oblate (22/166, 86.7%) and prolate (18/117, 84.6%) form primordial follicles. Our data suggest that the mechanical protocol effectively isolates viable preantral follicles at distinct differentiation stages from a limited thin area of the ovarian cortex.

Qualitative and quantitative morphological analysis

Morphological and morphometric analysis of the follicle population in cortical ovarian tissue punch samples was preceded by the assessment of the effectiveness in the bovine species of a previously consolidated protocol in humans, mice, and sheep (Adeniran, et al. 2021). The protocol aimed to reduce bias introduced by technical artifacts and, consequently, misinterpretation of morphological structures and to increase accuracy in estimating follicle reserve.

Biopsies were randomly excised from 20x10 mm in size and 0.5 to 1 mm thick ovarian cortex strips isolated from ovaries of 12 unselected animals were fixed in Form-Acetic and NBF for 16 hours and 24 hours, then processed and stained with H&E. Analyses were conducted on 27 histological sections per condition to assess stroma integrity and on 99 and 95 follicles for NBF (16 hours and 24 hours, respectively), and 119 and 139 follicles for Form-Acetic (16 hours and 24 hours, respectively) to assess follicle integrity. As reported in Fig. 4, the histological analysis indicates that Form-Acetic better preserves ovarian tissue morphology than NBF, also in the bovine species. Fixation in Form-Acetic resulted in a significantly lower level of tissue artifacts and greater stroma integrity than NBF, both for 16 and 24 hours (Fig. 4 A, B). Similarly, also concerning the morphological structures, our findings indicate that Form-Acetic ensures a significantly lower level of follicle artifacts than NBF, thus better preserving follicle integrity (Fig. 4 C, D). When comparing the fixation duration, no differences were observed between Form-Acetic fixation for 16 and 24 hours.

The morphometric analysis of the biopsy punch ovarian cortex revealed the presence of a population of preantral follicles, from primordial to early secondary, characterized by a significant increase in diameter, as shown in Fig. 5 and Supplementary Table 1. Follicle dimensions, assessed by calculating the mean of two perpendicular and diagonal measurements in follicles that contained a cross-section of the oocyte nucleus, were slightly inferior to those determined in freshly isolated counterparts. The smaller dimensions, however, similar to those described in previous histological studies, are attributed to the treatment of fixation of the tissues, as already reported in the literature (Borges, et al. 2023, Chatterjee 2014, Sarma, et al. 2020).

Moreover, the transition from the primordial to the secondary follicle stage is characterized by a significant increase in oocyte and oocyte nucleus diameter (Fig. 5 E, F).

Effect of age on preantral follicle density, follicle yield rate, and efficiency

The characterization of the preantral follicle population in individuals of different ages and the assessment of the follicular density to extrapolate the efficiency according to the extent of the ovarian reserve was conducted on a total of 14 heifers and 17 cows in 7 independent experiments. To determine follicle density in the two different ages, biopsy punch samples from heifers and cows were fixed for 24 hours in Form-Acetic and then processed for morphometric assessment. The follicle population was analyzed to evaluate the follicle density per mm^3 and yield rate after mechanical isolation based on the strip volume in individuals of different ages, adjusted for biopsy thickness. As reported in Fig. 6, the strip thickness utilized for mechanical follicle isolation and the assessment of follicle density includes zones from 1 to 4 that contain most of the preantral follicle populations, as previously described (van Wezel and Rodgers 1996). The depth of biopsies conducted on heifers and cows expressed as mean ± SEM was 797.6 ± 59.2 µm, without differences between the two ages (768.1 ± 111.1 vs. 827.2 ± 52.3, respectively, $p = 0.6406$).

Follicle density was calculated as described above and expressed as the number of follicles of each category per mm^3 (Fig. 7). The number of healthy primordial follicles was significantly lower in cows than in heifers. At the same time, no differences were shown in primary and early secondary follicles. Moreover, no differences were observed in the number of atretic follicles in each category. Furthermore, our data indicate that the prolate primordial follicle population represents one-third of the total primordial follicle category.

After the mechanical isolation procedure, the overall preantral follicle yield rate was significantly higher in heifers than in cows (653.25±279.71 and 105.91±89.85, mean ± SD, $p<0.05$). As reported in Fig. 8, the average of primordial and primary follicles retrieved from a 20x10 mm strip of the ovarian cortex was significantly higher in heifers than in cows. In evaluating the follicle isolation rate, the primordial follicles comprise both oblate and prolate forms. At the same time, no differences were observed in the early secondary follicle population retrieval between the two individuals' ages.

Finally, ovary weight, width, length, and the calculation of isolation efficiency are reported in Supplementary Table 2. Ovary dimensions were used to calculate the surface of the ovarian cortex that is exploitable for follicle recovery in individuals of different ages (see discussion). The preantral follicle isolation efficiencies for both heifers and cows have individually been calculated by proportionating the number of follicles retrieved through the mechanical isolation procedure (follicle/mm^3) against the follicle density (follicle/mm^3) (Table 1).

Discussion

Replicating the entire process of folliculogenesis in vitro in mammals still represents a highly demanding and ambitious breakthrough (reviewed in (Gosden and Yin 2013, Paulino, et al. 2022, Telfer, et al. 2023)). According to the species, the whole span of follicle growth in vivo ranges from 3 weeks in mice (Faddy, et al. 1983) to 6 months or more in humans and cows (Gougeon 1986, Lussier, et al. 1987). Such lengthy periods are not unusual when culturing homogeneous cell lines, while it is challenging for follicles composed of at least two cell types that cannot be considered a homogeneous population, particularly when cultured in a fragment of the ovarian cortex. Regarding the heterogeneity of the preantral follicle population, deciphering the peculiarities distinctive of each stage represents a crucial node to define ad-hoc protocols for in vitro follicle growth. The characterization of each stage and the definition of multi-step protocols to support the specific needs of each phase are mandatory to carry out the long folliculogenesis path in vitro. A multi-step method used in cattle and humans (McLaughlin, et al. 2018, McLaughlin, et al. 2010) provided proof of concept in large mammals but remained far from offering a personalized approach in fertility preservation interventions.

In the present study, we provide the rationale of a practical approach to maximizing the recovery rate of primordial, primary, and early secondary follicles from a limited portion of the ovarian cortex in the bovine model. In the first part of the study, we refined a protocol of mechanical isolation of primordial, primary, and secondary follicles from a limited portion of the ovarian cortex in the bovine model, starting from the state-of-the-art procedures and adopting specific methodological strategies for its optimization. The first strategy was to consider the thickness of the ovarian cortex, where preantral follicles concentrate. The ovarian cortex comprises discrete zones from 1 to 5 (Fig. 6). Zones 1 to 4 are substantially avascular and rich in collagen fibrils, containing primordial to early secondary follicles (van Wezel and Rodgers 1996). Zone 1 is represented by the surface epithelium, a single layer of cuboidal or elongated cells parallel to the surface of the ovary. Just beneath, Zones 2 to 4

mainly include from primordial and up to the early secondary follicle stage near Zone 5, which marks the passage in the vascularized area where large antral follicles are harbored (van Wezel and Rodgers 1996). Notably, we took into consideration a depth of 500-800 µm, which covers 1 - 4 zones, mainly containing follicles from the primordial up to the early secondary follicle stage (Fig. 6). As expected, the mechanical isolation procedure effectively isolates homogeneous primordial, primary, and early secondary follicle sub-populations from the homogenate of the ovarian cortex. Freshly isolated follicle measurements indicate the progressive increase in size from primordial to early antral follicle stage, and measures were consistent with those already reported on isolated bovine follicles (Candelaria and Denicol 2020, Hulshof, et al. 1994, Langbeen, et al. 2015).

With respect to the primordial follicles, the present study isolated the individual oblate and prolate primordial follicle forms from the ovarian cortex for the first time. The oblate form is frequent in the bovine ovary and has been described utilizing light microscopy and electron microscopy (Fair, et al. 1997, van Wezel and Rodgers 1996). The prolate form has been interpreted to be primordial follicles with an ellipsoid shape imposed upon them by the surrounding bundles of collagen fibrils (van Wezel and Rodgers 1996). An intermediate, prolate form has also been observed in humans (Gougeon and Chainy 1987), in which some granulosa cells (usually on one side of the follicle) are cuboidal in shape (Fig. 1 in (Gougeon and Chainy 1987)). These follicles are often as numerous as the spherical primordial follicles but with more granulosa cells seen in cross-sections (Gougeon and Chainy 1987). Moreover, in the African elephant, they are named early primary follicles and are described as oocytes surrounded by a single layer of pregranulosa cells, some of which are cuboidal in shape (Stansfield, et al. 2011). Interestingly, early primary follicles represent almost 80% of the ovarian reserve, while true primordial follicles, represented by an oocyte surrounded by a single layer of flat pregranulosa cells, form less than 2% of the follicle reserve (Stansfield, et al. 2011).

The commonly used terms 'transitional' or 'intermediate' (Rice, et al. 2008, Stubbs, et al. 2007, Westergaard, et al. 2007), which are often used to describe these follicles, can be

potentially misleading if they are used to mean that these follicles are in a transition stage from primordial to primary. As suggested by Rodgers et al., (Rodgers and Irving-Rodgers 2010a), primordial follicles that have been activated but not yet developed to the primary stage would be expected to be very few unless characterized by a slow rate of cell division, which is improbable to be the case as evidenced by studies conducted in rat (Meredith, et al. 2000). For this reason, the terms intermediate or transitional should not necessarily mean a transition from primordial to primary follicle. We have characterized the presence of oblate and prolate forms in histological and morphometric analyses and through mechanical isolation. Our data further confirm the above hypothesis. As indicated by the morphometric analysis, the population of the prolate shape represented in the analyses conducted both in heifers and cows was about a third of the population of primordial follicles (Fig. 7). However, isolating and characterizing the two forms of primordial follicles in the bovine model taps into a further novelty of this study. It opens the opportunity to deepen the investigation of the two forms of primordial follicles identified in humans, cattle, rats, and elephants, decipher their physiological role in follicle reserve establishment, and dissect the molecular events in a phase that preceded the primordial follicle activation (Hummitzsch, et al. 2015).

Another methodological refinement was the adoption of serial filtrations through 300, 100, 70, 40, and 30 µm decreasing mesh sizes strainers that allowed for isolating a homogeneous population of early secondary, primary, and primordial follicles with minimum debris. Filtering through the 30 µm mesh size strainer separates the primordial follicles by eliminating the residues of stroma cells that cause reaggregation, thus isolating a clean and homogeneous population.

The overall follicle viability after mechanical isolation was almost 70%, more elevated than previously reported (Langbeen, et al. 2015) with a significantly higher percentage of vital follicles in the primordial class (84.7%), compared to 55.1% and 63.8% in primary and early secondary follicles, respectively.

In the morphological analyses, our data confirms and expands the efficacy of the Form-Acetic-based fixative protocol in the bovine species. Initially tested in humans, sheep, and mice (Adeniran, et al. 2021), the method improved morphological preservation of bovine ovarian tissue in the present study, thus reducing biased evaluation of stroma organization and follicle developmental stages. The use of Form-Acetic significantly reduced stroma artifacts and follicle alterations. In general, measures of the follicle population were similar to those reported in the literature, even if morphometric assessments on serial histological sections indicated a slight reduction of the follicle structures compared to those previously described (Braw-Tal and Yossefi 1997, Hulshof, et al. 1994, van Wezel and Rodgers 1996). Although this may be due to the different fixation methods utilized in the other studies, there is no choral agreement in the dimensions, even in the literature. Nevertheless, the morphometric analysis indicates a significant increase in follicle and oocyte dimensions during the primordial to secondary follicle transition. Interestingly, as for freshly isolated follicles, morphometry highlighted significant differences between oblate and prolate in follicle diameter and oocyte and oocyte nucleus diameters asking for further studies to characterize this transition.

The second part of the study aimed to define the effectiveness of the isolation protocol, considering the individual's age as a critical factor, bearing in mind the progressive decrease in the ovarian reserve that physiologically accompanies the reproductive lifespan. Our results demonstrate a significant age-related reduction of the ovarian reserve in the comparison between 12 to 24-month heifers and 40 to 87-month-old cows. Based on the follicle density in 1 mm^3 of the ovarian cortex, the morphometric analysis indicated a 70.2% decrease in the overall preantral follicle population in cows (71.25 ± 61.14) compared to heifers (239.11 ± 96.79) (Table 1) confirming a halving of the ovarian reserve reported in previous studies (Modina, et al. 2014, Silva-Santos, et al. 2011). This reduction correlates well with the accelerated loss of follicles in women from 38 years of age onwards (Faddy and Gosden 1996).

The reduction of cows' ovarian reserve also affected the number of preantral follicles recovered after mechanical isolation. As indicated in Fig. 8, the number of isolated primordial and primary follicles was significantly lower in cows than in heifers.

Considering the yield rate per mm^3, starting from a fragment 20x10 mm in size and 0.8 mm in thickness (0.16 cm^3), we obtained an average of 4.08 and 0.67 preantral follicles in heifers and cows, respectively (Table 1).

In addition to the decrease in ovarian reserve, another factor that could affect the follicle recovery rate is the stroma's stiffness, which is consequent to an age-associated increase in the collagen fibers and hyaluronan matrices in the ovarian cortex (Amargant, et al. 2020, Ouni, et al. 2021, Shen, et al. 2023).

Regardless of the isolation protocol adopted, yield rate has been occasionally reported in previous studies, more often the overall number of recovered preantral follicles from several ovaries or cumulative ovarian tissue samples. Considering the population of preantral follicles estimated by morphometric analysis in the two age individuals per mm^3 (Fig. 7), the refined mechanical isolation protocol retrieved 10.54% and 4.69% preantral follicles from heifers and cow’s ovaries, respectively (Table 1). Interestingly, our data indicate that the refined protocol provides a yield rate considerably higher than previously reported, irrespective of the isolation protocol adopted. For example, in bovine, using mechanical isolation protocol, Langbeen et al. reported a yield rate of 0.04 preantral follicles/mm^3 (Jorssen, et al. 2015), while enzymatic isolation protocols using collagenase yielded about 0.19 preantral follicle/mm^3 from bovine biopsy (Aerts, et al. 2008). In human ovarian biopsies, using enzymatic isolation (liberase or collagenase), an average of 0.57 follicles/mm^3 (Vanacker, et al. 2011) and a range of 0.27 to 2.72 of preantral follicles/mm^3 variable according to the sample (Dolmans, et al. 2006) were recovered.

Benchmarking the follicle recovery rate from a well-defined fragment of the ovarian cortex based on biological parameters can provide tools to finely plan fertility conservation interventions. In the present study, we introduced this aspect by quantifying the follicles for the mm^3 unit of ovarian cortex obtained with an improved mechanical isolation protocol, and

we compared it with the preantral follicle population morphometrically measured in the same volume of the ovarian cortex. This framework offers the possibility of refining rescue interventions of the ovarian cortex through ultrasound-guided biopsy collection, as indicated by previous studies conducted in cows (Aerts, et al. 2008, Aerts, et al. 2005), mares (Haag, et al. 2013a, b), and in humans (Kagawa, et al. 2009, Rice, et al. 2008). Finally, age, follicle distribution within individuals and between species represent a further variable to consider, as beyond the intrinsic heterogeneity in the distribution of the populations of preantral follicles in the ovary as described in human (Schmidt, et al. 2003) and bovine (Gonzalez, et al. 2023), peculiar differences of species, such as in the mare, where the preantral follicles are located mainly close to the ovulatory fossa must be taken into account (Alves, et al. 2018, Hyde, et al. 2022). Furthermore, our approach suggests sampling of the cortex, which is richer in preantral follicles, avoiding the medulla region, which is poor in preantral follicles. The engraving for a depth of 0.8 mm and an area of 20x10 mm on the ovarian surface can significantly decrease invasiveness and secure organ function maintenance, as previously demonstrated with repeated periodic ovarian biopsies in the same individual in cows (Aerts, et al. 2008).

Starting from the extent of the ovarian reserve and the similarities in the composition and morphology of the primordial follicle population, our study further emphasizes the bovine species as a comparative model. Bovine and human reproductive biology share many similarities (Sirard 2017). Cows and women have similar folliculogenesis length (Gosden and Telfer 1987, Gougeon, et al. 1994, Lussier, et al. 1987, van den Hurk and Zhao 2005), are monovular, cycle continuously while not pregnant, have a gestation period of approximately 9 months, and their ovaries are similar in size (about 3 cm × 2 cm × 1.5 cm), morphology (Adams and Pierson 1995), architecture (Kagawa, et al. 2009, Nikniaz, et al. 2021), and are similar in structure and stroma composition (Campbell, et al. 2003, Roberts and Jeff Huang 2022, Sirard 2017).

In conclusion, our study provides a high-yield strategy for the mechanical isolation of preantral follicle populations from a limited quantity of the ovarian cortex, thus preserving the organ function and minimizing the invasiveness of the interventions, therefore allowing the designing of quantitative and conservative fertility preservation approaches from an age-related perspective. Maximizing the rescue of preantral follicles can boost the advancement in the development of in vitro follicle systems with promising approaches such as 3D systems, as recently suggested in mice (Converse, et al. 2023) and humans (Grubliauskaite, et al. 2024), thus providing a powerful means to further exploit the female reproductive potential. Finally, the refined isolation protocol provides a unique tool for studying folliculogenesis physiology and investigating the molecular blueprint of the crucial stages of early folliculogenesis, thus deciphering the sophisticated machinery that orchestrates mammalian follicular differentiation crucial for developing in vitro growth systems.

Declaration of interest

The authors declare that no conflict of interest could be perceived as prejudicing the impartiality of the research reported.

Fundings

This work was supported by Regione Lombardia FEASR - Programma di Sviluppo Rurale 2014-2020, Sottomisura 10.2 - “Sostegno per la conservazione, l’uso e lo sviluppo sostenibili delle risorse genetiche in agricoltura” - Operazione 10.2.01 - “Conservazione della biodiversità animale e vegetale” No. 202102146691 (R-INNOVA), the Italian Ministry of University and Research (MUR), PRIN2020, No. 20209L8BN4 (InfinitEGG), and by European Union's Horizon 2020 Marie Skłodowska-Curie Innovative Training Network, grant agreement No. 860960 ("EUROVA").

This study was also carried out within the Agritech National Research Center and received funding from the European Union Next-GenerationEU (PIANO NAZIONALE DI RIPRESA E RESILIENZA (PNRR) – MISSIONE 4 COMPONENTE 2, INVESTIMENTO 1.4 – D.D. 1032 17/06/2022, CN00000022). This manuscript reflects only the authors' views and opinions. Neither the European Union nor the European Commission can be considered responsible for them.

PD fellowship is supported by funding from the European Union's Horizon 2020 Marie Skłodowska-Curie Innovative Training Network, grant agreement No. 860960 ("EUROVA"); NM fellowship is funded by PON MUR doctorate. NK was supported by the EU's Erasmus+ Traineeship program to the Democritus University of Thrace, Greece

Author contribution statement

AML, PD, and NM conceived the study. NM, PD, LD, NK, and AML performed the experiments. NM, LD, and NK conducted the independent morphological and morphometric assessments. The manuscript was drafted by NM and PD, written by AML, and revised by

VL and FF. All authors discussed the results, analyzed data, and contributed to the final manuscript.

Acknowledgments

The authors thank INALCA S.p.A. (Ospedaletto Lodigiano, LO), Mr. Gianluca Pesatori, Dr. Massimo Sinelli, and the veterinary staff for their valuable support.

This work is dedicated to Professor Antonio Lauria with gratitude; his creativity and thoughts are still motivating. The preantral follicle isolation experiments in the middle 90s, with a drill and a blender blade, inspired and guided our imagination in perceiving the ovary's magnificent landscapes.

651 **Figure Captions**

652

653 **Figure 1.** A schematic representation of the mechanical isolation workflow. A strip of 2 cm^2
654 and between 0.5 to 1 mm thick of ovarian cortex was cut from the ovary surface (a), carefully
655 minced (b), washed (c), and homogenized (d). The homogenate was passed through
656 strainers with different mesh sizes (e). Strainers of 70 µm, 40 µm, and 30 µm were flipped
657 and washed (f) to recover early secondary, primary, and primordial follicles, respectively.
658 Created with BioRender.com (Certificate issued February 18, 2024).

659

660 **Figure 2.** Representative images of freshly isolated bovine preantral follicles after
661 mechanical isolation procedure. Follicles were classified based on their morphology as
662 primordial oblate, PMFo (A), primordial prolate, PMFp (B), primary, PF (C), and early
663 secondary, SF (D). Scale bar = 50 µm. Follicle diameters (E) were analyzed using the
664 Kruskal-Wallis test, followed by Dunn's multiple comparisons test. Data are expressed as
665 mean ± SD; *, and **** indicate significant differences ($p<0.05$, and $p<0.0001$, respectively).

666

667 **Figure 3.** (A) Representative phase contrast and fluorescence microscopy images of
668 different stage bovine follicles stained by dual-fluorescence assay using Fluorescein
669 Diacetate (FDA, green, live cells) and propidium iodide (PI, red, dead cells). Scale bar = 100
670 µm. (B) Representative phase contrast and fluorescence microscopy images (PI/FDA) at
671 higher magnification. Scale bar = 50 µm. Follicles were classified into two categories
672 depending on the percentage of dead granulosa cells and oocyte viability. Specifically,
673 Follicles were classified as live when oocyte and granulosa cells were all viable or with
674 <10% dead cells, while they were considered dead when with >10% dead cells. White
675 arrowheads indicate follicles evaluated as dead, and yellow arrowhead points to a single
676 dead granulosa cell within a viable primordial follicle. (C) Graphical representation of follicle
677 viability. Data from different animals (n = 12) were analyzed with the ANOVA test followed by

678 Tukey’s test; numerical values were represented as the mean percentage ± SEM.
679 **indicates a significant difference ($p<0.01$).
680
681
682 **Figure 4.** Representative images of H&E-stained bovine ovarian sections fixed with NBF
683 and Form-Acetic for 16h and 24h to evaluate artifacts affecting stroma (A, B) and follicle
684 integrity (C, D) to avoid compromising the morphological assessment. Stroma artifacts (A)
685 are represented by the detachment of stromal cells one from the other (asterisk), follicle
686 artifacts (C) are characterized by the receding away of follicles from the stroma (yellow
687 arrowhead), shrunken ooplasm within oocytes (green arrowhead), oocyte nuclei
688 condensation (red arrowhead). Scale bar = 100 µm. The bar graphs represent the
689 percentage area of stroma artifacts (B) and the percentage of follicles showing artifacts (D)
690 for the two fixatives (NBF in black, Form-Acetic in grey).
691 Data from five independent experiments (n=5) were analyzed for stroma artifact with the
692 Kruskal-Wallis test followed by Dunn's test and for follicle artifact with Ordinary one-way
693 ANOVA followed by Tukey’s test; numerical values were represented as the mean ± SEM;
694 **** indicate significant differences ($p<0.0001$).
695
696 **Figure 5.** Representative images of bovine follicles in H&E histological sections fixed with
697 Form-Acetic for 24h. Follicles were classified based on their morphology as primordial
698 oblate, PMFo (A), primordial prolate, PMFp (B), primary, PF (C), and early secondary, SF
699 (D). Scale bar = 50 µm. Oocyte (E) and oocyte nucleus (F) diameter data were analyzed
700 using the Kruskal-Wallis test, followed by Dunn's multiple comparisons test. Data are
701 expressed as mean ± SD; *, ***, and **** indicate significant differences ($p<0.05$, $p<0.001$
702 and $p<0.0001$, respectively).
703
704 **Figure 6.** Longitudinal sections through three representative bovine ovaries, showing zones
705 1–5 organization. Zone 1, the surface epithelium, comprised a single layer of cuboidal cells

parallel to the ovary surface, lying on the extracellular matrix. Zones 2 and 3 are the outer and inner regions of Tunica albuginea, and their width can vary. Cells in Zone 2 are spindle-shaped and parallel to the surface epithelium, whereas cells in Zone 3 are more rounded and irregular in orientation; in both zones, cells are separated apart by many collagen fibers. Zone 4 contains collagen fibers and a more significant number of preantral follicles. Zone 5 corresponds to the medulla area, which includes large antral follicles. Arrowheads indicate blood vessels. Scale bar = 100 µm.

Figure 7. Effect of the age on the bovine preantral follicle density. The bar graph represents the follicle number in 1 mm^3 of the ovarian cortex collected from heifers (black bars) and cows (grey bars). Follicles from primordial (PMF) are subdivided into primordial oblate (histogram with solid pattern), primordial prolate (histogram with downward diagonal stripes), primary (PF), and early secondary (SF). All stages are subdivided into healthy and atretic. Data were analyzed by 2-way ANOVA followed by Šidák's test; data are expressed as mean ± SD; **** indicates significant differences ($p<0.0001$).

Figure 8. Effect of age on the isolation rate of bovine primordial (PMF), primary (PF), and early secondary (SF) follicles. The bar graph represents the number of follicles isolated from a 20x10 mm ovarian cortex fragment from heifers (black bars) and cows (grey bars). Data were analyzed by 2-way ANOVA followed by Sidak's test; data are expressed as mean ± SD; **** indicates significant differences ($p<0.0001$).

References

Adams, GP, and RA Pierson 1995 Bovine model for study of ovarian follicular dynamics in humans. *Theriogenology* **43** 113-120.

Adeniran, BV, BD Bjarkadottir, R Appeltant, S Lane, and SA Williams 2021 Improved preservation of ovarian tissue morphology that is compatible with antigen detection using a fixative mixture of formalin and acetic acid. *Human reproduction* **36** 1871-1890.

Aerts, J, B Martinez-Madrid, K Flothmann, J De Clercq, S Van Aelst, and P Bols 2008 Quantification and viability assessment of isolated bovine primordial and primary ovarian follicles retrieved through a standardized biopsy pick-up procedure. *Reprod Domest Anim* **43** 360-366.

Aerts, JM, M Oste, and PE Bols 2005 Development and practical applications of a method for repeated transvaginal, ultrasound-guided biopsy collection of the bovine ovary. *Theriogenology* **64** 947-957.

Alves, BG, KA Alves, GDA Gastal, MO Gastal, JR Figueiredo, and EL Gastal 2018 Spatial distribution of preantral follicles in the equine ovary. *PLoS One* **13** e0198108.

Amargant, F, SL Manuel, Q Tu, WS Parkes, F Rivas, LT Zhou, JE Rowley, CE Villanueva, JE Hornick, GS Shekhawat, JJ Wei, ME Pavone, AR Hall, MT Pritchard, and FE Duncan 2020 Ovarian stiffness increases with age in the mammalian ovary and depends on collagen and hyaluronan matrices. *Aging Cell* **19** e13259.

Amin, RU, K Chandrashekar Reddy, K Sadasiva Rao, KBP Raghavender, A Teja, T Ramesh, and G Arunakumari 2013 In vitro culture of goat preantral follicles from fetal ovaries. *Small Ruminant Research* **115** 71-76.

Araujo, VR, MO Gastal, JR Figueiredo, and EL Gastal 2014 In vitro culture of bovine preantral follicles: a review. *Reproductive biology and endocrinology : RB&E* **12** 78.

Araujo, VR, MO Gastal, A Wischral, JR Figueiredo, and EL Gastal 2015 Long-term in vitro culture of bovine preantral follicles: Effect of base medium and medium replacement methods. *Anim Reprod Sci* **161** 23-31.

Barboni, B, V Russo, S Cecconi, V Curini, A Colosimo, ML Garofalo, G Capacchietti, O Di Giacinto, and M Mattioli 2011 In vitro grown sheep preantral follicles yield oocytes with normal nuclear-epigenetic maturation. *PLoS One* **6** e27550.

Barros, VRP, APO Monte, T Lins, JM Santos, VG Menezes, AYP Cavalcante, VR Araujo, BB Gouveia, and MHT Matos 2019 In vitro survival, growth, and maturation of sheep oocytes from secondary follicles cultured in serum-free conditions: impact of a constant or a sequential medium containing recombinant human FSH. *Domest Anim Endocrinol* **67** 71-79.

Bezerra, FTG, FEO Lima, L Paulino, BR Silva, AWB Silva, ALP Souza, R van den Hurk, and JRV Silva 2019 In vitro culture of secondary follicles and prematuration of cumulus-oocyte complexes from antral follicles increase the levels of maturation-related transcripts in bovine oocytes. *Mol Reprod Dev* **86** 1874-1886.

Bjarkadottir, BD, CA Walker, M Fatum, S Lane, and SA Williams 2021 Analysing culture methods of frozen human ovarian tissue to improve follicle survival. *Reproduction and Fertility* **2** 59-68.

Borges, MA, BR Curcio, GDA Gastal, L Gheno, ASV Junior, CD Corcini, CEW Nogueira, FLN Aguiar, and EL Gastal 2023 Ethanol, Carnoy, and paraformaldehyde as fixative solutions for histological evaluation of preantral follicles in equine ovarian tissue. *Reprod Biol* **23** 100814.

Braw-Tal, R, and S Yossefi 1997 Studies in vivo and in vitro on the initiation of follicle growth in the bovine ovary. *J Reprod Fertil* **109** 165-171.

Bus, A, A Langbeen, B Martin, J Leroy, and PEJ Bols 2019 Is the pre-antral ovarian follicle the 'holy grail'for female fertility preservation? *Anim Reprod Sci* **207** 119-130.

Campbell, BK, C Souza, J Gong, R Webb, N Kendall, P Marsters, G Robinson, A Mitchell, EE Telfer, and DT Baird 2003 Domestic ruminants as models for the

783 elucidation of the mechanisms controlling ovarian follicle development in humans.
784 *Reprod Suppl* **61** 429-443.
785 **Candelaria, JI, and AC Denicol** 2020 Characterization of isolated bovine preantral follicles
786 based on morphology, diameter and cell number. *Zygote* **28** 154-159.
787 **Candelaria, JI, MB Rabaglino, and AC Denicol** 2020 Ovarian preantral follicles are
788 responsive to FSH as early as the primary stage of development. *J Endocrinol* **247**
789 153-168.
790 **Chatterjee, S** 2014 Artefacts in histopathology. *J Oral Maxillofac Pathol* **18** S111-116.
791 **Converse, A, EJ Zaniker, F Amargant, and FE Duncan** 2023 Recapitulating
792 folliculogenesis and oogenesis outside the body: encapsulated in vitro follicle
793 growthdagger. *Biol Reprod* **108** 5-22.
794 **Dey, P, and AM Luciano** 2022 A century of programmed cell death in the ovary: a
795 commentary. *J Assist Reprod Genet* **39** 63-66.
796 **Dey, P, N Monferini, L Donadini, V Lodde, F Franciosi, and AM Luciano** 2024 Method of
797 Isolation and In Vitro Culture of Primordial Follicles in Bovine Animal Model. *Methods*
798 *Mol Biol* **2770** 171-182.
799 **Dolmans, MM, N Michaux, A Camboni, B Martinez-Madrid, A Van Langendonckt, SA**
800 **Nottola, and J Donnez** 2006 Evaluation of Liberase, a purified enzyme blend, for
801 the isolation of human primordial and primary ovarian follicles. *Human reproduction*
802 **21** 413-420.
803 **Duncan, FE, M Zelinski, AH Gunn, JE Pahnke, CL O'Neill, N Songsasen, RI Woodruff,**
804 **and TK Woodruff** 2016 Ovarian tissue transport to expand access to fertility
805 preservation: from animals to clinical practice. *Reproduction* **152** R201-R210.
806 **Erickson, BH** 1966a Development and radioresponse of the prenatal bovine ovary. *J*
807 *Reprod Fertil* **11** 97-105.
808 **Erickson, BH** 1966b Development and senescence of the postnatal bovine ovary. *J Anim*
809 *Sci* **25** 800-805.

Faddy, MJ, and RG Gosden 1996 A model conforming the decline in follicle numbers to the age of menopause in women. *Human reproduction* **11** 1484-1486.

Faddy, MJ, RG Gosden, and RG Edwards 1983 Ovarian follicle dynamics in mice: a comparative study of three inbred strains and an F1 hybrid. *J Endocrinol* **96** 23-33.

Fair, T, SC Hulshof, P Hyttel, T Greve, and M Boland 1997 Oocyte ultrastructure in bovine primordial to early tertiary follicles. *Anat Embryol (Berl)* **195** 327-336.

Figueiredo, JR, SC Hulshof, R Van den Hurk, FJ Ectors, RS Fontes, B Nusgens, MM Bevers, and JF Beckers 1993 Development of a combined new mechanical and enzymatic method for the isolation of intact preantral follicles from fetal, calf and adult bovine ovaries. *Theriogenology* **40** 789-799.

Findlay, JK, KJ Hutt, M Hickey, and RA Anderson 2015 How Is the Number of Primordial Follicles in the Ovarian Reserve Established? *Biol Reprod* **93** 111.

Forabosco, A, and C Sforza 2007 Establishment of ovarian reserve: a quantitative morphometric study of the developing human ovary. *Fertil Steril* **88** 675-683.

Ford, EA, EL Beckett, SD Roman, EA McLaughlin, and JM Sutherland 2020 Advances in human primordial follicle activation and premature ovarian insufficiency. *Reproduction* **159** R15-R29.

Garcia Barros, R, V Lodde, F Franciosi, and AM Luciano 2023 A refined culture system of oocytes from early antral follicles promotes oocyte maturation and embryo development in cattle. *Reproduction* **165** 221-233.

Gonzalez, SM, MB Cerezetti, LZ Bergamo, F Morotti, and MM Seneda 2023 Spatial distribution of preantral follicles in ovarian parenchyma of bovine species. *Zygote* **31** 195-200.

Gosden, R, and H Yin 2013 In vitro growth and differentiation of oocytes. *In* U Eichenlaub-Ritter, R Gosden, and A Trounson (ed.), Biology and Pathology of the Oocyte: Role in Fertility, Medicine and Nuclear Reprograming, edn 2, pp. 187-199. Cambridge: Cambridge University Press.

Gosden, RG, and E Telfer 1987 Numbers of follicles and oocytes in mammalian ovaries and their allometric relationships. *J Zool* **211** 169-175.

Gougeon, A 1986 Dynamics of follicular growth in the human: a model from preliminary results. *Human reproduction* **1** 81-87.

Gougeon, A, and GB Chainy 1987 Morphometric studies of small follicles in ovaries of women at different ages. *J Reprod Fertil* **81** 433-442.

Gougeon, A, R Ecochard, and JC Thalabard 1994 Age-related changes of the population of human ovarian follicles: increase in the disappearance rate of non-growing and early-growing follicles in aging women. *Biol Reprod* **50** 653-663.

Grubliauskaite, M, H Vlieghe, S Moghassemi, A Dadashzadeh, A Camboni, Z Gudleviciene, and CA Amorim 2024 Influence of ovarian stromal cells on human ovarian follicle growth in a 3D environment. *Hum Reprod Open* **2024** hoad052.

Haag, KT, DM Magalhaes-Padilha, GR Fonseca, A Wischral, MO Gastal, SS King, KL Jones, JR Figueiredo, and EL Gastal 2013a Equine preantral follicles obtained via the Biopsy Pick-Up method: histological evaluation and validation of a mechanical isolation technique. *Theriogenology* **79** 735-743.

Haag, KT, DM Magalhaes-Padilha, GR Fonseca, A Wischral, MO Gastal, SS King, KL Jones, JR Figueiredo, and EL Gastal 2013b Quantification, morphology, and viability of equine preantral follicles obtained via the Biopsy Pick-Up method. *Theriogenology* **79** 599-609.

Hansen, KR, NS Knowlton, AC Thyer, JS Charleston, MR Soules, and NA Klein 2008 A new model of reproductive aging: the decline in ovarian non-growing follicle number from birth to menopause. *Human reproduction* **23** 699-708.

Hornick, JE, FE Duncan, LD Shea, and TK Woodruff 2013 Multiple follicle culture supports primary follicle growth through paracrine-acting signals. *Reproduction* **145** 19-32.

Hulshof, SC, JR Figueiredo, JF Beckers, MM Bevers, and R van den Hurk 1994 Isolation and characterization of preantral follicles from foetal bovine ovaries. *Vet Q* **16** 78-80.

Hummitzsch, K, RA Anderson, D Wilhelm, J Wu, EE Telfer, DL Russell, SA Robertson, and RJ Rodgers 2015 Stem cells, progenitor cells, and lineage decisions in the ovary. *Endocr Rev* **36** 65-91.

Hyde, KA, FLN Aguiar, BG Alves, KA Alves, GDA Gastal, MO Gastal, and EL Gastal 2022 Preantral follicle population and distribution in the horse ovary. *Reprod Fertil* **3** 90-102.

Ireland, JL, D Scheetz, F Jimenez-Krassel, AP Themmen, F Ward, P Lonergan, GW Smith, GI Perez, AC Evans, and JJ Ireland 2008 Antral follicle count reliably predicts number of morphologically healthy oocytes and follicles in ovaries of young adult cattle. *Biol Reprod* **79** 1219-1225.

Jachter, SL, WP Simmons, C Estill, J Xu, and CV Bishop 2022 Matrix-free three-dimensional culture of bovine secondary follicles to antral stage: Impact of media formulation and epidermal growth factor (EGF). *Theriogenology* **181** 89-94.

Jimenez, CR, VR Araujo, JM Penitente-Filho, JL de Azevedo, RG Silveira, and CA Torres 2016 The base medium affects ultrastructure and survival of bovine preantral follicles cultured in vitro. *Theriogenology* **85** 1019-1029.

Jorssen, EP, A Langbeen, WF Marei, E Fransen, HF De porte, JL Leroy, and PE Bols 2015 Morphologic characterization of isolated bovine early preantral follicles during short-term individual in vitro culture. *Theriogenology* **84** 301-311.

Kagawa, N, S Silber, and M Kuwayama 2009 Successful vitrification of bovine and human ovarian tissue. *Reprod Biomed Online* **18** 568-577.

Langbeen, A, EP Jorssen, E Fransen, AP Rodriguez, MC Garcia, JL Leroy, and PE Bols 2015 Characterization of freshly retrieved preantral follicles using a low-invasive, mechanical isolation method extended to different ruminant species. *Zygote* **23** 683-694.

Langbeen, A, EP Jorssen, N Granata, E Fransen, JL Leroy, and PE Bols 2014 Effects of neutral red assisted viability assessment on the cryotolerance of isolated bovine preantral follicles. *J Assist Reprod Genet* **31** 1727-1736.

Lazzari, G, C Galli, and RM Moor 1992 Centrifugal elutriation of porcine oocytes isolated from the ovaries of newborn piglets. *Anal Biochem* **200** 31-35.

Lonergan, P, and T Fair 2008 In vitro-produced bovine embryos: dealing with the warts. *Theriogenology* **69** 17-22.

Luciano, AM, RG Barros, ACS Soares, J Buratini, V Lodde, and F Franciosi 2021 Recreating the Follicular Environment: A Customized Approach for In Vitro Culture of Bovine Oocytes Based on the Origin and Differentiation State. *Methods Mol Biol* **2273** 1-15.

Luciano, AM, D Corbani, V Lodde, I Tessaro, F Franciosi, JJ Peluso, and S Modina 2011 Expression of progesterone receptor membrane component-1 in bovine reproductive system during estrous cycle. *Eur J Histochem* **55** e27.

Luciano, AM, F Franciosi, RG Barros, C Dieci, and V Lodde 2018 The variable success of in vitro maturation: can we do better? *Anim Reprod* **15** 727-736.

Luciano, AM, and MA Sirard 2018 Successful in vitro maturation of oocytes: a matter of follicular differentiation. *Biol Reprod* **98** 162-169.

Lussier, JG, P Matton, and JJ Dufour 1987 Growth rates of follicles in the ovary of the cow. *J Reprod Fertil* **81** 301-307.

Marcozzi, S, V Rossi, A Salustri, M De Felici, and FG Klinger 2018 Programmed cell death in the human ovary. *Minerva Ginecol* **70** 549-560.

McDonnell, SP, JI Candelaria, AJ Morton, and AC Denicol 2022 Isolation of Small Preantral Follicles from the Bovine Ovary Using a Combination of Fragmentation, Homogenization, and Serial Filtration. *J Vis Exp*.

McGee, EA, and AJ Hsueh 2000 Initial and cyclic recruitment of ovarian follicles. *Endocr Rev* **21** 200-214.

McLaughlin, M, DF Albertini, WHB Wallace, RA Anderson, and EE Telfer 2018 Metaphase II oocytes from human unilaminar follicles grown in a multi-step culture system. *Mol Hum Reprod* **24** 135-142.

McLaughlin, M, JJ Bromfield, DF Albertini, and EE Telfer 2010 Activin promotes follicular integrity and oogenesis in cultured pre-antral bovine follicles. *Mol Hum Reprod* **16** 644-653.

Meredith, S, G Dudenhoeffer, and K Jackson 2000 Classification of small type B/C follicles as primordial follicles in mature rats. *J Reprod Fertil* **119** 43-48.

Modina, SC, I Tessaro, V Lodde, F Franciosi, D Corbani, and AM Luciano 2014 Reductions in the number of mid-sized antral follicles are associated with markers of premature ovarian senescence in dairy cows. *Reprod Fertil Dev* **26** 235-244.

Nikniaz, H, Z Zandieh, M Nouri, N Daei-Farshbaf, R Aflatoonian, M Gholipourmalekabadi, and SB Jameie 2021 Comparing various protocols of human and bovine ovarian tissue decellularization to prepare extracellular matrix-alginate scaffold for better follicle development in vitro. *BMC Biotechnol* **21** 8.

O'Brien, MJ, JK Pendola, and JJ Eppig 2003 A revised protocol for in vitro development of mouse oocytes from primordial follicles dramatically improves their developmental competence. *Biol Reprod* **68** 1682-1686.

Ouni, E, A Peaucelle, KT Haas, O Van Kerk, MM Dolmans, T Tuuri, M Otala, and CA Amorim 2021 A blueprint of the topology and mechanics of the human ovary for next-generation bioengineering and diagnosis. *Nat Commun* **12** 5603.

Paulino, LFRM, EIT de Assis, VAN Azevedo, BR Silva, EV da Cunha, and JRV Silva 2022 Why Is It So Difficult To Have Competent Oocytes from In vitro Cultured Preantral Follicles? *Reprod Sci* **29** 3321-3334.

Rice, S, K Ojha, and H Mason 2008 Human ovarian biopsies as a viable source of pre-antral follicles. *Human reproduction* **23** 600-605.

Roberts, JF, and CC Jeff Huang 2022 Bovine models for human ovarian diseases. *Prog Mol Biol Transl Sci* **189** 101-154.

Rodgers, RJ, and HF Irving-Rodgers 2010a Formation of the ovarian follicular antrum and follicular fluid. *Biol Reprod* **82** 1021-1029.

Rodgers, RJ, and HF Irving-Rodgers 2010b Morphological classification of bovine ovarian follicles. *Reproduction* **139** 309-318.

Rueden, CT, J Schindelin, MC Hiner, BE DeZonia, AE Walter, ET Arena, and KW Eliceiri 2017 ImageJ2: ImageJ for the next generation of scientific image data. *BMC Bioinformatics* **18** 529.

Santos, SS, MA Ferreira, JA Pinto, RV Sampaio, AC Carvalho, TV Silva, NN Costa, MS Cordeiro, MS Miranda, HF Ribeiro, and OM Ohashi 2013 Characterization of folliculogenesis and the occurrence of apoptosis in the development of the bovine fetal ovary. *Theriogenology* **79** 344-350.

Sarma, UC, AL Winship, and KJ Hutt 2020 Comparison of methods for quantifying primordial follicles in the mouse ovary. *J Ovarian Res* **13** 121.

Schmidt, KL, AG Byskov, A Nyboe Andersen, J Muller, and C Yding Andersen 2003 Density and distribution of primordial follicles in single pieces of cortex from 21 patients and in individual pieces of cortex from three entire human ovaries. *Human reproduction* **18** 1158-1164.

Schneider, CA, WS Rasband, and KW Eliceiri 2012 NIH Image to ImageJ: 25 years of image analysis. *Nat Methods* **9** 671-675.

Shen, L, J Liu, A Luo, and S Wang 2023 The stromal microenvironment and ovarian aging: mechanisms and therapeutic opportunities. *J Ovarian Res* **16** 237.

Silva-Santos, KC, GM Santos, LS Siloto, MF Hertel, ER Andrade, MI Rubin, L Sturion, FA Melo-Sterza, and MM Seneda 2011 Estimate of the population of preantral follicles in the ovaries of Bos taurus indicus and Bos taurus taurus cattle. *Theriogenology* **76** 1051-1057.

Simon, LE, TR Kumar, and FE Duncan 2020 In vitro ovarian follicle growth: a comprehensive analysis of key protocol variables. *Biol Reprod* **103** 455-470.

Sirard, MA 2017 The ovarian follicle of cows as a model for human. *In* H Schatten and GM Constantinescu (ed.), Animal Models and Human Reproduction: Cell and Molecular Approaches with Reference to Human Reproduction, pp. 127-144. Wiley-Blackwell.

Stansfield, FJ, HM Picton, and JO Nothling 2011 Early primary--rather than primordial follicles constitute the main follicular reserve in the African elephant (Loxodonta africana). *Anim Reprod Sci* **123** 112-118.

Stubbs, SA, J Stark, SM Dilworth, S Franks, and K Hardy 2007 Abnormal preantral folliculogenesis in polycystic ovaries is associated with increased granulosa cell division. *J Clin Endocrinol Metab* **92** 4418-4426.

Telfer, EE 2019 FERTILITY PRESERVATION: Progress and prospects for developing human immature oocytes in vitro. *Reproduction* **158** F45-F54.

Telfer, EE, J Grosbois, YL Odey, R Rosario, and RA Anderson 2023 Making a good egg: human oocyte health, aging, and in vitro development. *Physiol Rev* **103** 2623-2677.

Telfer, EE, K Sakaguchi, YL Clarkson, and M McLaughlin 2019 In vitro growth of immature bovine follicles and oocytes. *Reprod Fertil Dev* **32** 1-6.

Tessaro, I, AM Luciano, F Franciosi, V Lodde, D Corbani, and SC Modina 2011 The endothelial nitric oxide synthase/nitric oxide system is involved in the defective quality of bovine oocytes from low mid-antral follicle count ovaries. *J Anim Sci* **89** 2389-2396.

Tilly, JL 2001 Commuting the death sentence: how oocytes strive to survive. *Nat Rev Mol Cell Biol* **2** 838-848.

van den Hurk, R, and J Zhao 2005 Formation of mammalian oocytes and their growth, differentiation and maturation within ovarian follicles. *Theriogenology* **63** 1717-1751.

van Wezel, IL, and RJ Rodgers 1996 Morphological characterization of bovine primordial follicles and their environment in vivo. *Biol Reprod* **55** 1003-1011.

Vanacker, J, A Camboni, C Dath, A Van Langendonckt, MM Dolmans, J Donnez, and CA Amorim 2011 Enzymatic isolation of human primordial and primary ovarian

follicles with Liberase DH: protocol for application in a clinical setting. *Fertil Steril* **96** 379-383 e373.

Vilela, JMV, MM Dolmans, and CA Amorim 2021 Ovarian tissue transportation: a systematic review. *Reprod Biomed Online* **42** 351-365.

Walker, CA, BD Bjarkadottir, M Fatum, S Lane, and SA Williams 2021 Variation in follicle health and development in cultured cryopreserved ovarian cortical tissue: a study of ovarian tissue from patients undergoing fertility preservation. *Hum Fertil (Camb)* **24** 188-198.

Westergaard, CG, AG Byskov, and CY Andersen 2007 Morphometric characteristics of the primordial to primary follicle transition in the human ovary in relation to age. *Human reproduction* **22** 2225-2231.

Wright, CS, O Hovatta, R Margara, G Trew, RM Winston, S Franks, and K Hardy 1999 Effects of follicle-stimulating hormone and serum substitution on the in-vitro growth of human ovarian follicles. *Human reproduction* **14** 1555-1562.

Xu, J, and MB Zelinski 2022 Oocyte quality following in vitro follicle development. *Biol Reprod* **106** 291-315.

1029

Figure 1

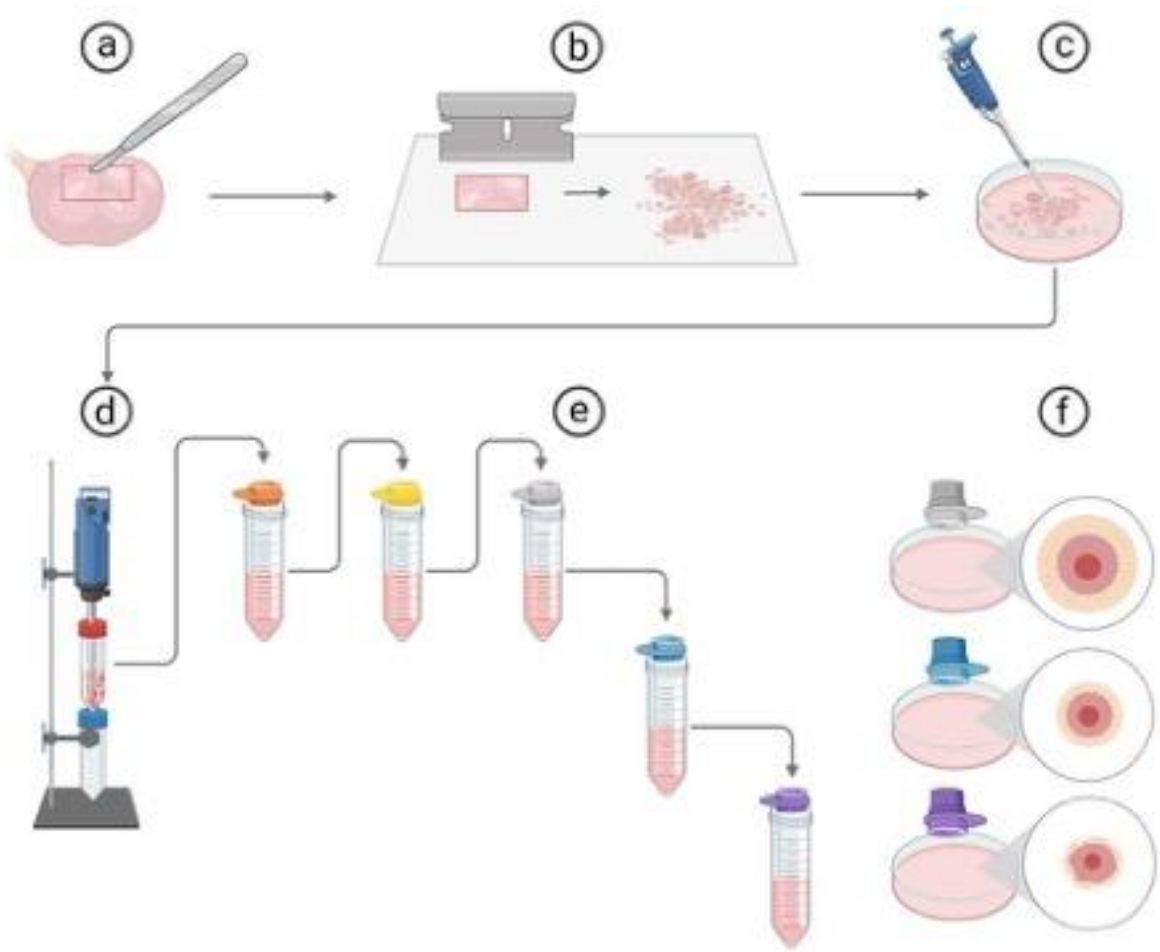

Figure 2

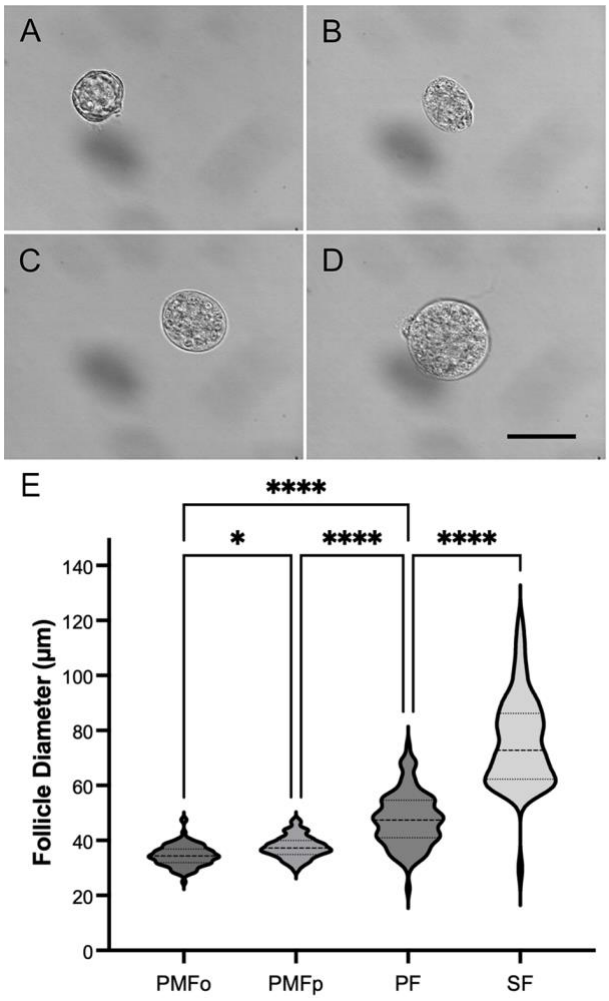
A
B
C
D
E
****
*
****
****
Follicle Diameter (µm)
0
20
40
60
80
100
120
140
PMFo
PMFp
PF
SF

Figure 3

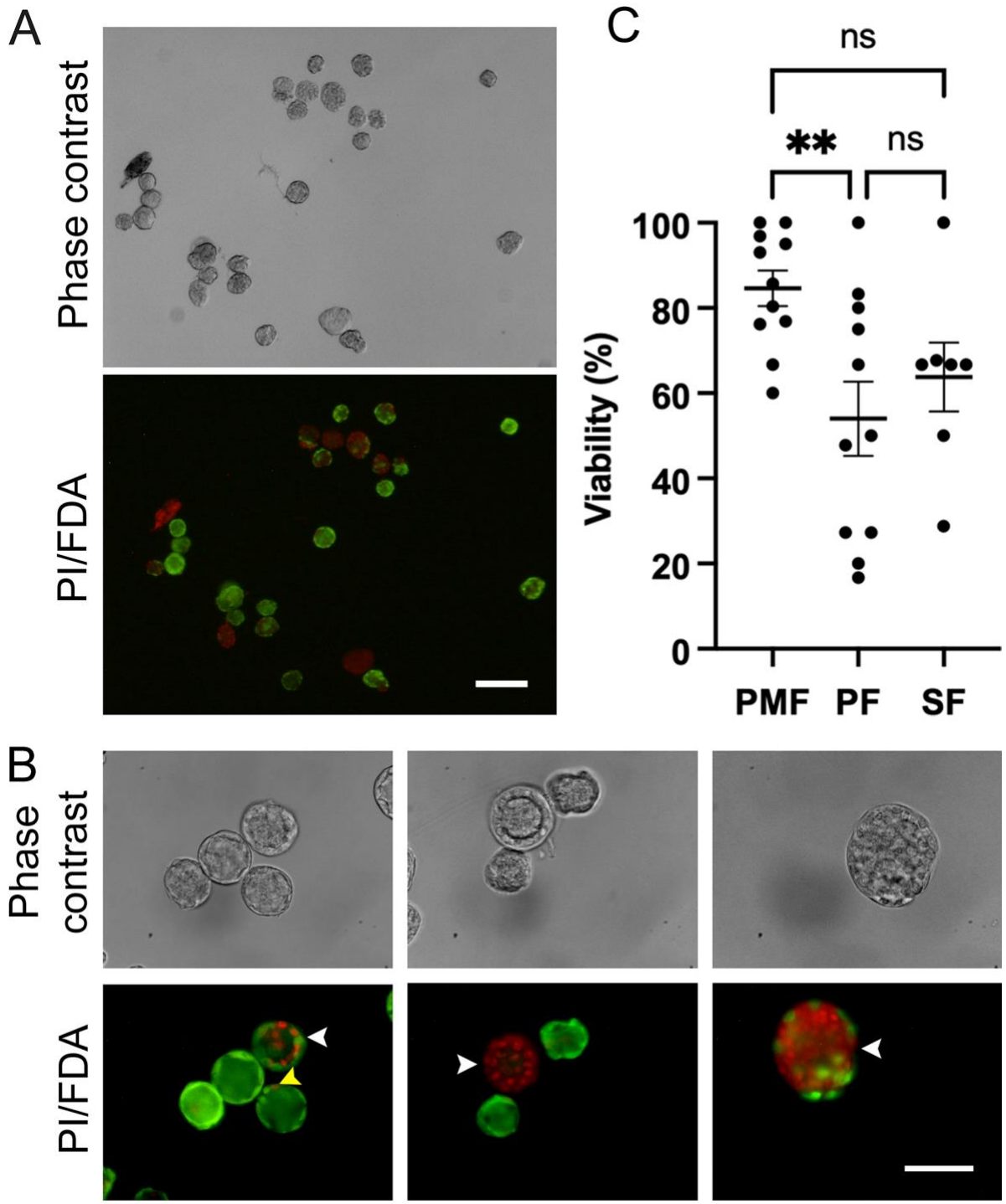
A
Phase contrast
PI/FDA
C
ns
**
ns
Viability (%)
100
80
60
40
20
0
PMF
PF
SF
B
Phase contrast
PI/FDA

Figure 4

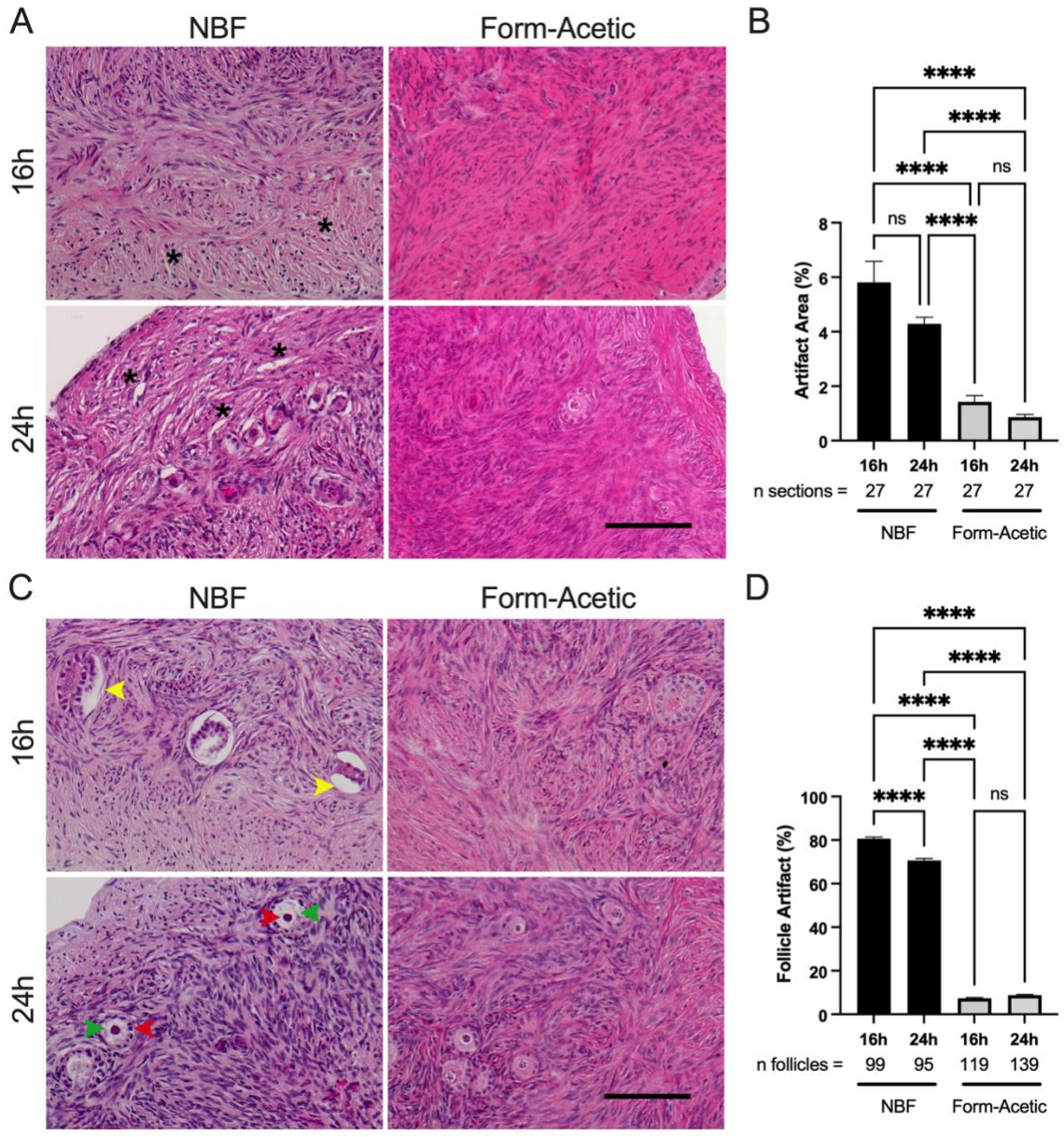
A
NBF
Form-Acetic
16h
24h
B
Artifact Area (%)
****
****
****
ns
ns
****
16h 24h 16h 24h
n sections = 27 27 27 27
NBF
Form-Acetic
C
NBF
Form-Acetic
16h
24h
D
Follicle Artifact (%)
****
****
****
****
****
ns
16h 24h 16h 24h
n follicles = 99 95 119 139
NBF
Form-Acetic

Figure 5

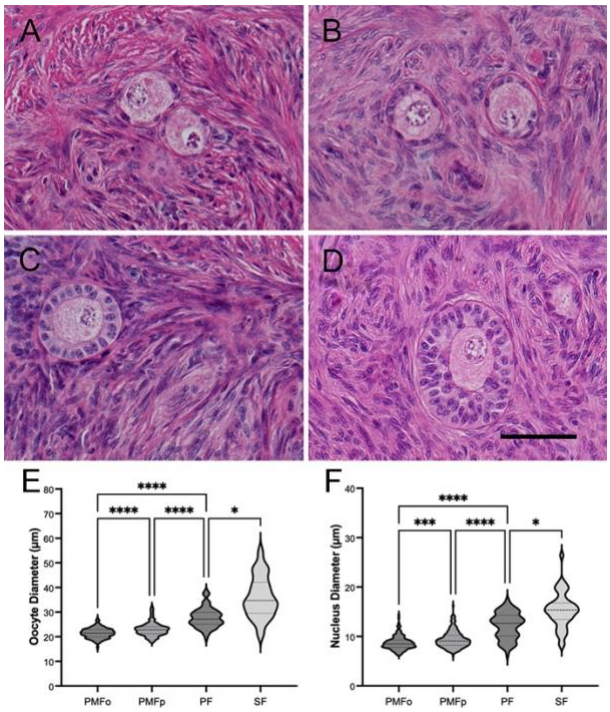
A
B
C
D
E
Oocyte Diameter (µm)
PMFo
PMFp
PF
SF
****
****
****
*
F
Nucleus Diameter (µm)
PMFo
PMFp
PF
SF
****
***
****
*

Figure 6

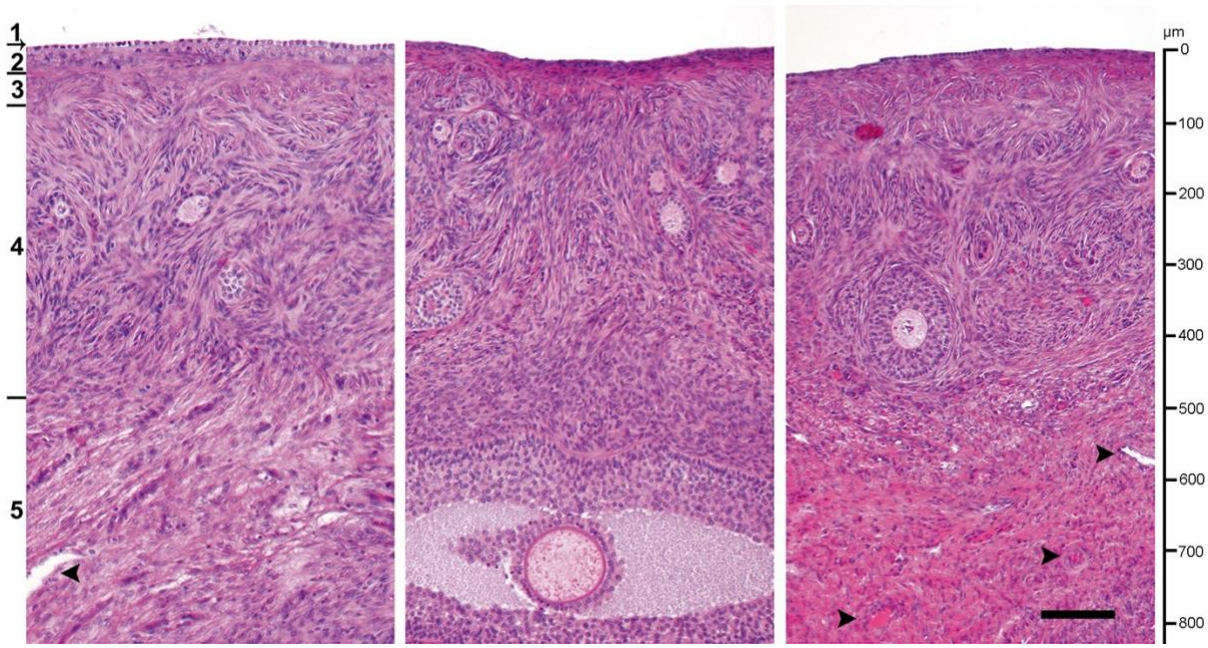

Figure 7

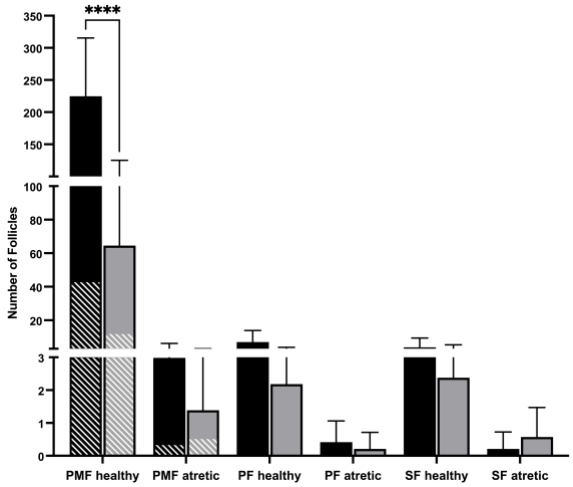

Figure 8

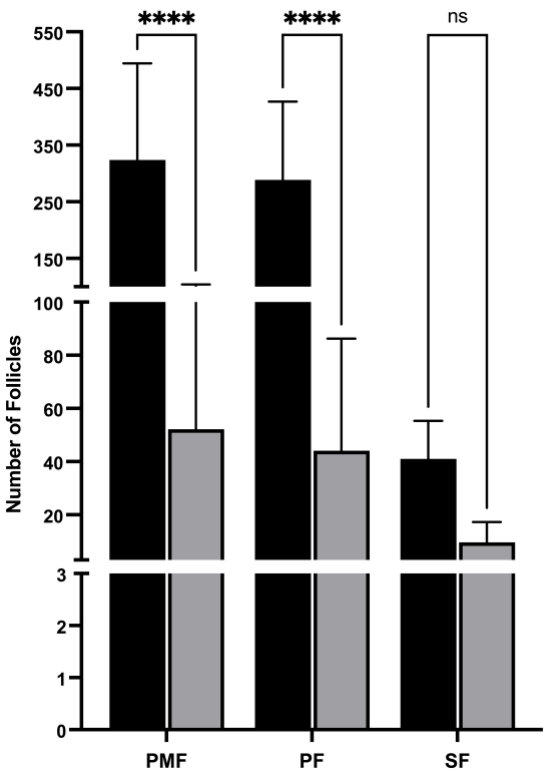
****
****
ns
550
450
350
250
150
100
80
60
40
20
3
2
1
0
Number of Follicles
PMF
PF
SF

1137

1138

Table 1. Efficiency of follicle isolation per volume of tissue by age. The isolation efficiency was evaluated by performing the ratio between the follicle density evaluated in 1 mm^3 of the ovarian cortex and the number of isolated PMF, PF, and SF per strip (10x20x0.8 mm, 0.16 cm^3), then expressed in 1 mm^3 in the two age groups.

	Heifers				Cows			
	PMF	PF	SF	Total (Preantral)	PMF	PF	SF	Total (Preantral)
Follicle density[1] (follicles/mm^3 ovarian cortex)	227.67 ± 92.12	7.39 ± 6.95	4.05 ± 5.57	239.11 ± 104.64	65.91 ± 60.66	2.39 ± 1.65	2.95 ± 3.71	71.25 ± 66.02
Yield rate[1] (follicles/strip)	323.75 ± 170.40	288.50 ± 138.13	41.00 ± 14.29	653.25 ± 322.82	52.18 ± 56.43	44.09 ± 47.27	9.64 ± 7.49	105.91 ± 111.22
Yield rate[1] (follicles/mm^3)	2.02 ± 1.07	1.80 ± 0.86	0.26 ± 0.09	4.08 ± 2.02	0.33 ± 0.32	0.28 ± 0.26	0.06 ± 0.05	0.67 ± 0.63
Isolation efficiency[2] (yield rate per mm^3/follicle density per mm^3)	0.89	24.40	6.33	**10.54**	0.49	11.53	2.04	**4.69**

[1]Values are expressed as mean ± SD.

[2]Values are expressed as mean percentage

Supplementary Figure 1

Figure 1. (A) Representative image of an ovary and surface area calculation. The surface was estimated by approximating the ovary to an ellipse. The ellipse area was calculated by multiplying half of the height (h) and half of the length (l) by π. The resulting area was multiplied by two to obtain the total ovarian cortex surface. The approximate calculation of the ellipse area was verified using ImageJ NIH by tracing the outline of the ovary and measuring the area included. (B) Representative image of the ovarian cortical strip (20x10x0.8 mm) isolated from the ovary and utilized for preantral follicle isolation. (C) A representative example of a biopsy punch of 2 mm diameter excised from the strip to evaluate the follicle density enclosed in 1 mm^3. Scale bar = 1 cm.

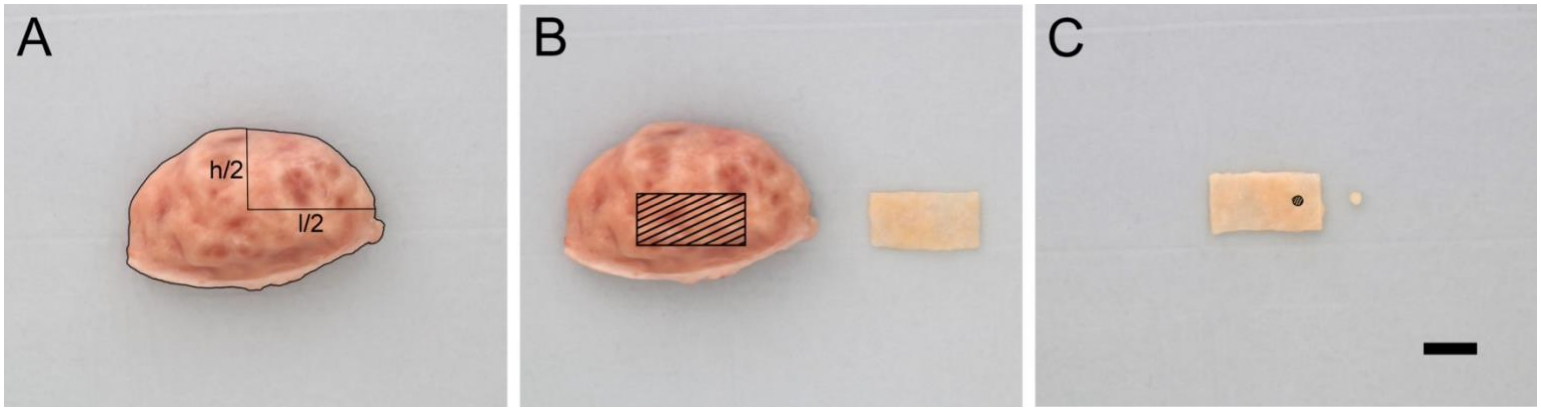

Supplementary Table 1

Table 1. Freshly isolated follicle diameter and follicle, oocyte, and oocyte nucleus diameter measured in 6 µm H&E histological sections of bovine ovarian cortex biopsies[1].

	Freshly isolated follicle		Histologically processed follicle			
Follicle	N	Follicle diameter (µm)	N	Follicle diameter (µm)	Oocyte diameter (µm)	Nucleus diameter (µm)
Primordial oblate	176	34.51 ± 3.79 [a]	260	28.41 ± 2.46 [a]	21.46 ± 2.06 [a]	8.69 ± 1.35 [a]
Primordial prolate	113	37.59 ± 3.97 [b]	220	33.30 ± 4.66 [b]	23.01 ± 2.75 [b]	9.39 ± 1.68 [b]
Primary	96	47.63 ± 9.71 [c]	78	46.78 ± 9.20 [c]	27.70 ± 4.00 [c]	12.20 ± 2.62 [c]
Early secondary	63	75.9 ± 16.4 [d]	44	79.55 ± 18.16 [d]	36.04 ± 8.32 [d]	15.35 ± 3.54 [d]

[1]Values are expressed as mean ± SD. Data with different superscripts in the same column differ significantly (from $p<0.05$ to $p<0.0001$; see Figures 2 and 5).

Supplementary Table 2

Table 2. Ovary weight and dimension by age. The surface area of the ovary was approximated to the ellipse area formula. Measurements were obtained from n=160 heifer ovaries (12-24 months old) and n=46 cow ovaries (40-87 months old). Data were analyzed by t-test with Welch correction, followed by Holm-Sidak test[1].

	Heifer	Cow	p value
Weight (g)	7.7 ± 3.2	13.0 ± 4.6	<0.000001
Length (cm)	3.1 ± 0.8	3.9 ± 0.8	<0.000001
Height (cm)	2.2 ± 0.5	2.8 ± 1.1	0.000738
Surface area (cm^2)	10.9 ± 3.9	17.3 ± 7.8	0.000002

[1]Values are expressed as mean ± SD.